Ain Shams Engineering Journal (2014) 5, 489–503

Ain Shams University
Ain Shams Engineering Journal
www.elsevier.com/locate/asej
www.sciencedirect.com

ENGINEERING PHYSICS AND MATHEMATICS

Effects of Hall current, radiation and rotation on natural convection heat and mass transfer flow past a moving vertical plate

G.S. Seth [a,*], S. Sarkar [a], S.M. Hussain [b]

[a] Department of Applied Mathematics, Indian School of Mines, Dhanbad 826004, India
[b] Department of Mathematics, OP Jindal Institute of Technology, Raigarh 496109, India

Received 20 July 2013; revised 31 August 2013; accepted 26 September 2013
Available online 28 October 2013

KEYWORDS
Natural convection;
Hall current;
Coriolis force;
Ramped temperature;
Optically thick radiating fluid

Abstract An investigation of the effects of Hall current and rotation on unsteady hydromagnetic natural convection flow with heat and mass transfer of an electrically conducting, viscous, incompressible and optically thick radiating fluid past an impulsively moving vertical plate embedded in a fluid saturated porous medium, when temperature of the plate has a temporarily ramped profile, is carried out. Exact solution of the governing equations is obtained in closed form by Laplace transform technique. Exact solution is also obtained in case of unit Schmidt number. Expressions for skin friction due to primary and secondary flows and Nusselt number are derived for both ramped temperature and isothermal plates. Expression for Sherwood number is also derived. The numerical values of primary and secondary fluid velocities, fluid temperature and species concentration are displayed graphically whereas those of skin friction are presented in tabular form for various values of pertinent flow parameters.

1. Introduction

Natural convection flow induced by thermal and solutal buoyancy forces acting over bodies with different geometries in a fluid saturated porous medium is prevalent in many natural phenomena and has varied and wide range of industrial applications. For example, in atmospheric flows, the presence of pure air or water is impossible because some foreign mass may be present either naturally or mixed with air or water due to industrial emissions. Natural processes such as attenuation of toxic waste in water bodies, vaporization of mist and fog, photosynthesis, drying of porous solids, transpiration, sea-wind formation (where upward convection is modified by Coriolis forces), and formation of ocean currents [1] occur due to thermal and solutal buoyancy forces developed as a result of difference in temperature or concentration or a combination of these two. Such configuration is also encountered in several practical systems for industry based applications viz. heat exchanger devices, cooling of molten metals, insulation systems, petroleum reservoirs, filtration,

* Corresponding author. Mobile: +91 9006482450.
E-mail address: gsseth_ism@yahoo.com (G.S. Seth).
Peer review under responsibility of Ain Shams University.

ELSEVIER Production and hosting by Elsevier

2090-4479 © 2013 Production and hosting by Elsevier B.V. on behalf of Ain Shams University.
http://dx.doi.org/10.1016/j.asej.2013.09.014

Nomenclature

B_0	uniform magnetic field
c_p	specific heat at constant pressure
g	acceleration due to gravity
G_c	solutal Grashof number
K'_1	permeability of porous medium
k^*	Rosseland mean absorption coefficient
m	Hall current parameter
N	thermal radiation parameter
q'_r	radiative flux vector
T'	fluid temperature
U_0	uniform velocity of the plate
w'	fluid velocity in z' direction
C'	species concentration
D	chemical molecular diffusivity
G_r	thermal Grashof number
k	thermal conductivity of the fluid
K_1	permeability parameter
K^2	rotation parameter
M^2	magnetic parameter
P_r	Prandtl number
S_c	Schmidt number
t_0	characteristic time
u'	fluid velocity in x' direction

Greek symbols

β'	volumetric coefficient of thermal expansion
β^*	volumetric coefficient of expansion for species concentration
ρ	fluid density
σ^*	Stefan–Boltzmann constant
τ_e	electron collision time
Ω	uniform angular velocity
σ	electrical conductivity
ν	kinematic coefficient of viscosity
ω_e	cyclotron frequency

chemical catalytic reactors and processes, nuclear waste repositories, desert coolers, wet bulb thermometers, frost formation in vertical channels, etc. Considering the importance of such fluid flow problems, extensive and in-depth research works have been carried out by several researchers [2–10] in the past. Comprehensive reviews of natural convection boundary layer flow over various geometrical bodies with heat and mass transfer in porous and non-porous media are well documented by Eckert and Drake [11], Gebhart et al. [12], Nield and Bejan [13], Pop and Ingham [14] and Incropera et al. [15].

Investigation of hydromagnetic natural convection flow with heat and mass transfer in porous and non-porous media has drawn considerable attentions of several researchers owing to its applications in astrophysics, geophysics, aeronautics, electronics, meteorology, metallurgy, chemical and petroleum industries. Magnetohydrodynamic (MHD) natural convection flow of an electrically conducting fluid in a fluid saturated porous medium has also been successfully exploited in crystal formation. Oreper and Szekely [16] have found that the presence of a magnetic field can suppress natural convection currents and the strength of magnetic field is one of the important factors in reducing non-uniform composition thereby enhancing quality of the crystal. In addition to it, the thermal physics of hydromagnetic problems with mass transfer is of much significance in MHD energy generators, MHD flow-meters, MHD pumps, MHD accelerators, controlled thermo-nuclear reactors, etc. Keeping in view the importance of such study, Hossain and Mandal [17] investigated mass transfer effects on unsteady hydromagnetic free convection flow past an accelerated vertical porous plate. Jha [18] studied hydromagnetic free convection and mass transfer flow past a uniformly accelerated vertical plate through a porous medium when magnetic field is fixed with the moving plate. Elbashbeshy [19] discussed heat and mass transfer along a vertical plate in the presence of magnetic field. Chen [20] analyzed combined heat and mass transfer in MHD free convection flow from a vertical surface with Ohmic heating and viscous dissipation. Ibhrahim et al. [21] considered unsteady MHD micropolar fluid flow and heat transfer past a vertical porous plate through a porous medium in the presence of thermal and mass diffusions with a constant heat source. Chamkha [22] investigated unsteady MHD convection flow with heat and mass transfer past a semi-infinite vertical permeable moving plate in a uniform porous medium with heat absorption. Makinde and Sibanda [23] investigated MHD mixed convection flow with heat and mass transfer past a vertical plate embedded in a uniform porous medium with constant wall suction in the presence of uniform transverse magnetic field. Makinde [24] studied MHD mixed convection flow and mass transfer past a vertical porous plate embedded in a porous medium with constant heat flux. Eldabe et al. [25] discussed unsteady MHD flow of a viscous and incompressible fluid with heat and mass transfer in a porous medium near a moving vertical plate with time-dependent velocity.

Investigation of hydromagnetic natural convection flow in a rotating medium is of considerable importance due to its application in various areas of geophysics, astrophysics and fluid engineering viz. maintenance and secular variations in Earth's magnetic field due to motion of Earth's liquid core, internal rotation rate of the Sun, structure of the magnetic stars, solar and planetary dynamo problems, turbo machines, rotating MHD generators, rotating drum separators for liquid metal MHD applications, etc. It may be noted that Coriolis and magnetic forces are comparable in magnitude and Coriolis force induces secondary flow in the flow-field. Taking into consideration the importance of such study, unsteady hydromagnetic natural convection flow past a moving plate in a rotating medium is studied by a number of researchers. Mention may be made of research studies of Singh [26,27], Raptis and Singh [28], Kythe and Puri [29], Tokis [30], Nanousis [31] and Singh et al. [32].

In all these investigations, the effects of thermal radiation are not taken into account. However, thermal radiation effects on hydromagnetic natural convection flow with heat and mass transfer play an important role in manufacturing processes taking place in industries for the design of fins, glass production, steel rolling, casting and levitation, furnace design, etc.

Moreover, several engineering processes occur at very high temperatures where the knowledge of radiative heat transfer becomes indispensible for the design of pertinent equipment. Nuclear power plants, gas turbines and various propulsion devices for aircraft, missiles, satellites and space vehicles are examples of such engineering areas [33]. It is worthy to note that unlike convection/conduction the governing equations taking into account the effects of thermal radiation become quite complicated. Hence many difficulties arise while solving such equations. However, some reasonable approximations are proposed to solve the governing equations with radiative heat transfer. Viskanta and Grosh [34] were one of the initial investigators to study the effects of thermal radiation on temperature distribution and heat transfer in an absorbing and emitting media flowing over a wedge. They used Rosseland approximation for the radiative flux vector to simplify the energy equation. Cess [35] studied laminar free convection along a vertical isothermal plate with thermal radiation. The text books by Sparrow and Cess [36] and Howell et al. [37] present the most essential features and state of the art applications of radiative heat transfer. Takhar et al. [38] analyzed the effects of radiation on MHD free convection flow of a gas past a semi-infinite vertical plate. Raptis and Massalas [39] studied oscillatory magnetohydrodynamic flow of a gray, absorbing-emitting fluid with non-scattering medium past a flat plate in the presence of radiation assuming the Rosseland flux model. Chamkha [40] discussed thermal radiation and buoyancy effects on hydromagnetic flow over an accelerating permeable surface with heat source or sink. Seddeek [33] studied effects of thermal radiation and variable viscosity on unsteady hydromagnetic natural convection flow past a semi-infinite flat plate with an aligned magnetic field. Cookey et al. [41] considered the influence of viscous dissipation and radiation on unsteady MHD free convection flow past an infinite heated vertical plate in a porous medium with time-dependent suction. Suneetha et al. [42] studied effects of thermal radiation on unsteady hydromagnetic free convection flow past an impulsively started vertical plate with variable surface temperature and concentration. Ogulu and Makinde [43] considered unsteady hydromagnetic free convection flow of a dissipative and radiative fluid past a vertical plate with constant heat flux. Mahmoud [44] investigated the effects of thermal radiation on unsteady MHD free convection flow past an infinite vertical porous plate taking into account the effects of viscous dissipation.

In all these investigations, analytical or numerical solution is obtained assuming conditions for fluid velocity and temperature at the plate as continuous and well defined. However, there exist several practical problems which may require non-uniform or arbitrary thermal conditions. Keeping in view this fact, several researchers investigated free convection flow from a vertical plate with step discontinuities in the surface temperature. Pioneering work is due to Schetz [45] who developed an approximate model for free convection flow from a vertical plate with discontinuous thermal boundary conditions. Later, several investigations were carried out on such fluid flow problems by using an experimental technique [46], numerical methods [47] and series expansion methods [48,49]. Lee and Yovanovich [50] developed a new analytical model for laminar natural convection flow past a vertical plate with a step change in wall temperature. Chandran et al. [51] analyzed unsteady natural convective flow of a viscous and incompressible fluid near a vertical plate with ramped temperature. Patra et al. [52] considered the effects of radiation on natural convection flow of a viscous and incompressible fluid near a stationary vertical flat plate with ramped temperature. Narahari [53] discussed unsteady free convection flow between two vertical plates with ramped temperature within one of the plates in the presence of thermal radiation and mass diffusion. Seth et al. [54] studied unsteady MHD natural convection flow with radiative heat transfer past an impulsively moving vertical plate with ramped temperature embedded in a fluid saturated porous medium with thermal diffusion. Recently, Seth et al. [55] considered the effects of rotation on unsteady hydromagnetic free convection flow of a viscous, incompressible and optically thick radiating fluid past an impulsively moving vertical plate with ramped temperature in a fluid saturated porous medium.

It is noticed that when the density of an electrically conducting fluid is low and/or applied magnetic field is strong, Hall current is produced in the flow-field which plays an important role in determining flow features of the problems because it induces secondary flow in the flow-field. Keeping in view this fact, significant investigations on hydromagnetic free convection flow past a flat plate with Hall effects under different thermal conditions are carried out by several researchers in the past. Mention may be made of the research studies of Pop and Watanabe [56], Abo-Eldahab and Elbarbary [57], Takhar et al. [58] and Saha et al. [59]. It is worthy to note that Hall current induces secondary flow in the flow-field which is also the characteristics of Coriolis force. Therefore, it becomes very important to compare and contrast the effects of these two agencies and also to study their combined effects on such fluid flow problems. Satya Narayana et al. [60] studied the effects of Hall current and radiation–absorption on MHD natural convection heat and mass transfer flow of a micropolar fluid in a rotating frame of reference. Seth et al. [61] investigated effects of Hall current and rotation on unsteady hydromagnetic natural convection flow of a viscous, incompressible, electrically conducting and heat absorbing fluid past an impulsively moving vertical plate with ramped temperature in a porous medium taking into account the effects of thermal diffusion.

Objective of the present investigation is to study the effects of Hall current and rotation on unsteady hydromagnetic natural convection flow with heat and mass transfer of a viscous, incompressible, electrically conducting and optically thick radiating fluid past an impulsively moving vertical plate embedded in a fluid saturated porous medium taking into account the effects of thermal and mass diffusions when temperature of the plate has a temporarily ramped profile. This problem has not yet received any attention from the researchers although natural convection heat and mass transfer flow resulting from such ramped temperature profile of a plate may have strong bearings on several engineering problems viz. in designing of electromagnetic devices, in high temperature aerodynamics, plasma physics, cosmical flight, nuclear power reactors, etc. where initial temperature profiles are of much significance and thermal radiation is highly prevalent.

2. Formulation of the problem and its solution

Consider unsteady hydromagnetic natural convection flow with heat and mass transfer of an electrically conducting, viscous, incompressible and optically thick radiating fluid past an infinite vertical plate embedded in a uniform porous medium in a rotating system taking Hall current into account. Coordinate system is chosen in such a way that x'-axis is considered along the plate in upward direction and y'-axis normal to plane of the plate in the fluid. A uniform transverse magnetic field B_0 is applied in a direction which is parallel to y'-axis. The fluid and plate rotate in unison with uniform angular velocity Ω about y'-axis. Initially i.e. at time $t' \leqslant 0$, both the fluid and plate are at rest and are maintained at a uniform temperature T'_∞. Also species concentration at the surface of the plate as well as at every point within the fluid is maintained at uniform concentration C'_∞. At time $t' > 0$, plate starts moving in x'-direction with uniform velocity U_0 in its own plane. The temperature of plate is raised or lowered to $T'_\infty + (T'_w - T'_\infty)t'/t_0$ when $0 < t' \leqslant t_0$, and it is maintained at uniform temperature T'_w when $t' > t_0$ (t_0 being characteristic time). Also, at time $t' > 0$, species concentration at the surface of the plate is raised to uniform species concentration C'_w and is maintained thereafter. Geometry of the problem is presented in Fig. 1. Since plate is of infinite extent in x' and z' directions and is electrically non-conducting, all physical quantities except pressure, depend on y' and t' only. Also no applied or polarized voltages exist so the effect of polarization of fluid is negligible. This corresponds to the case where no energy is added or extracted from the fluid by electrical means [62]. It is assumed that the induced magnetic field generated by fluid motion is negligible in comparison to the applied one. This assumption is justified because magnetic Reynolds number is very small for liquid metals and partially ionized fluids which are commonly used in industrial applications [62].

Keeping in view the assumptions made above, governing equations for natural convection flow with heat and mass transfer of an electrically conducting, viscous, incompressible and optically thick radiating fluid through a uniform porous medium in a rotating frame of reference taking Hall current into account, under Boussinesq approximation, are given by

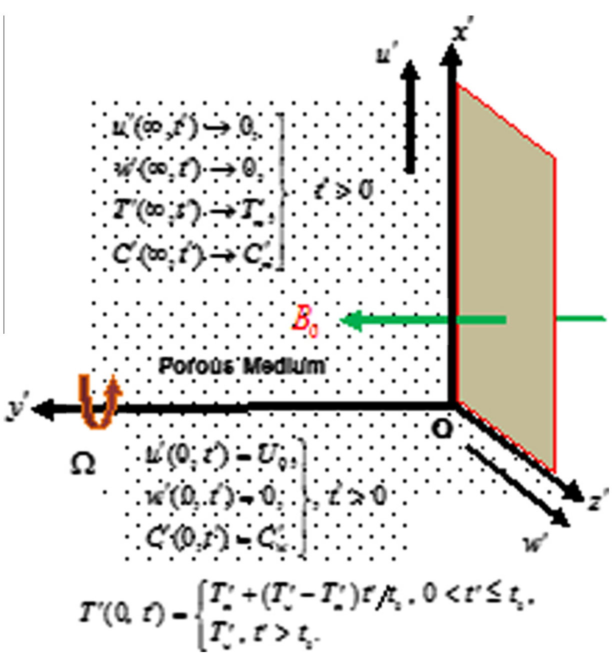

Figure 1 Geometry of the problem.

$$\frac{\partial u'}{\partial t'} + 2\Omega w' = \nu \frac{\partial^2 u'}{\partial y'^2} - \frac{\sigma B_0^2}{\rho(1+m^2)}(u' + mw') - \frac{\nu u'}{K_1'} + g\beta'(T' - T'_\infty) + g\beta^*(C' - C'_\infty), \quad (1)$$

$$\frac{\partial w'}{\partial t'} - 2\Omega u' = \nu \frac{\partial^2 w'}{\partial y'^2} + \frac{\sigma B_0^2}{\rho(1+m^2)}(mu' - w') - \frac{\nu w'}{K_1'}, \quad (2)$$

$$\rho c_p \frac{\partial T'}{\partial t'} = k \frac{\partial^2 T'}{\partial y'^2} - \frac{\partial q_r'}{\partial y'}, \quad (3)$$

$$\frac{\partial C'}{\partial t'} = D \frac{\partial^2 C'}{\partial y'^2}, \quad (4)$$

where u', w', ν, ρ, σ, $m = \omega_e \tau_e$, ω_e, τ_e, g, β', β^*, T', C', c_p, k, K_1', q_r' and D are, respectively, fluid velocity in x'-direction, fluid velocity in z'-direction, kinematic coefficient of viscosity, fluid density, electrical conductivity, Hall current parameter, cyclotron frequency, electron collision time, acceleration due to gravity, volumetric coefficient of thermal expansion, volumetric coefficient of expansion for species concentration, fluid temperature, species concentration, specific heat at constant pressure, thermal conductivity of the fluid, permeability of the porous medium, radiative flux vector and chemical molecular diffusivity.

Initial and boundary conditions for the fluid flow problem are specified below

$$u' = w' = 0, \quad T' = T'_\infty, \quad C' = C'_\infty \quad \text{for} \quad y' \geqslant 0 \quad \text{and} \quad t' \leqslant 0, \quad (5a)$$

$$u' = U_0, \quad w' = 0 \quad \text{at} \quad y' = 0 \quad \text{for} \quad t' > 0, \quad (5b)$$

$$T' = T'_\infty + (T'_w - T'_\infty)t'/t_0 \quad \text{at} \quad y' = 0 \quad \text{for} \quad 0 < t' \leqslant t_0, \quad (5c)$$

$$T' = T'_w \quad \text{at} \quad y' = 0 \quad \text{for} \quad t' > t_0, \quad (5d)$$

$$C' = C'_w \quad \text{at} \quad y' = 0 \quad \text{for} \quad t' > 0, \quad (5e)$$

$$u', \quad w' \to 0; \quad T' \to T'_\infty; \quad C' \to C'_\infty \quad \text{as} \quad y' \to \infty \quad \text{for} \quad t' > 0. \quad (5f)$$

For an optically thick fluid, in addition to emission there is also self-absorption and usually the absorption coefficient is wavelength dependent and large so we can adopt the Rosseland approximation for radiative flux vector q_r' [36]. Thus q_r' is given by

$$q_r' = -\frac{4\sigma^*}{3k^*}\frac{\partial T'^4}{\partial y'}, \quad (6)$$

where k^* is Rosseland mean absorption coefficient and σ^* is Stefan–Boltzmann constant. Assuming small temperature difference between fluid temperature T' and free stream temperature T'_∞, T'^4 is expanded in Taylor series about free stream temperature T'_∞ to linearize equation (6) which, after neglecting second and higher order terms in $(T' - T'_\infty)$, assumes the form

$$T'^4 \cong 4T'^3_\infty T' - 3T'^4_\infty. \quad (7)$$

Eq. (3) with help of Eqs. (6) and (7) reduces to

$$\frac{\partial T'}{\partial t'} = \frac{k}{\rho c_p}\frac{\partial^2 T'}{\partial y'^2} + \frac{1}{\rho c_p}\frac{16\sigma^* T'^3_\infty}{3k^*}\frac{\partial^2 T'}{\partial y'^2}. \quad (8)$$

Eqs. (1), (2), (4) and (8), in non-dimensional form, are presented in the following forms

$$\frac{\partial u}{\partial t} + 2K^2 w = \frac{\partial^2 u}{\partial y^2} - \frac{M^2}{(1+m^2)}(u + mw) - \frac{u}{K_1} + G_r T + G_c C, \tag{9}$$

$$\frac{\partial w}{\partial t} - 2K^2 u = \frac{\partial^2 w}{\partial y^2} + \frac{M^2}{(1+m^2)}(mu - w) - \frac{w}{K_1}, \tag{10}$$

$$\frac{\partial C}{\partial t} = \frac{1}{S_c}\frac{\partial^2 C}{\partial y^2}, \tag{11}$$

$$\frac{\partial T}{\partial t} = \frac{(1+N)}{P_r}\frac{\partial^2 T}{\partial y^2}, \tag{12}$$

where

$y = y'/U_0 t_0, \quad u = u'/U_0, \quad w = w'/U_0, \quad t = t'/t_0,$
$T = (T' - T'_\infty)/(T'_w - T'_\infty), \quad C = (C' - C'_\infty)/(C'_w - C'_\infty),$
$G_r = g\beta' \nu (T'_w - T'_\infty)/U_0^3, \quad G_c = g\beta^* \nu (C'_w - C'_\infty)/U_0^3,$
$M^2 = \sigma B_0^2 \nu/\rho U_0^2, \quad K^2 = \nu\Omega/U_0^2,$
$K_1 = K'_1 U_0^2/\nu^2, \quad P_r = \nu\rho c_p/k, \quad N = 16\sigma^* T_\infty^3/3kk^*$ and
$S_c = \nu/D.$

M^2, K^2, K_1, G_r, G_c, P_r, N and S_c are, respectively, magnetic parameter, rotation parameter, permeability parameter, thermal Grashof number, solutal Grashof number, Prandtl number, thermal radiation parameter and Schmidt number.

Characteristic time t_0 is defined according to the non-dimensional process mentioned above as $t_0 = \nu/U_0^2$.

Initial and boundary conditions (5a)-(5f), in non-dimensional form, are given by

$$u = w = 0, \quad T = 0, \quad C = 0 \quad \text{for} \quad y \geqslant 0 \quad \text{and} \quad t \leqslant 0, \tag{13a}$$

$$u = 1, \quad w = 0 \quad \text{at} \quad y = 0 \quad \text{for} \quad t > 0, \tag{13b}$$

$$T = t \quad \text{at} \quad y = 0 \quad \text{for} \quad 0 < t \leqslant 1, \tag{13c}$$

$$T = 1 \quad \text{at} \quad y = 0 \quad \text{for} \quad t > 1, \tag{13d}$$

$$C = 1 \quad \text{at} \quad y = 0 \quad \text{for} \quad t > 0, \tag{13e}$$

$$u \to 0, \quad w \to 0; \quad T \to 0; \quad C \to 0 \quad \text{as} \quad y \to \infty \quad \text{for} \quad t > 0. \tag{13f}$$

Eqs. (9) and (10) are presented, in compact form, as

$$\frac{\partial F}{\partial t} = \frac{\partial^2 F}{\partial y^2} - \lambda F + G_r T + G_c C, \tag{14}$$

where $F = u + iw$ and $\lambda = M^2(1 - im)/(1 + m^2) + 1/K_1 - 2iK^2$.

Initial and boundary conditions (13a)-(13f), in compact form, become

$$F = 0, \quad T = 0, \quad C = 0 \quad \text{for} \quad y \geqslant 0 \quad \text{and} \quad t \leqslant 0, \tag{15a}$$

$$F = 1, \quad \text{at} \quad y = 0 \quad \text{for} \quad t > 0, \tag{15b}$$

$$T = t \quad \text{at} \quad y = 0 \quad \text{for} \quad 0 < t \leqslant 1, \tag{15c}$$

$$T = 1 \quad \text{at} \quad y = 0 \quad \text{for} \quad t > 1, \tag{15d}$$

$$C = 1 \quad \text{at} \quad y = 0 \quad \text{for} \quad t > 0, \tag{15e}$$

$$F \to 0, \quad T \to 0, \quad C \to 0, \quad \text{as} \quad y \to \infty \quad \text{for} \quad t > 0. \tag{15f}$$

Eqs. (11), (12) and (14), after taking Laplace transform and using initial conditions (15a), reduce to

$$\frac{d^2\overline{T}}{dy^2} - sa\overline{T} = 0, \tag{16}$$

$$\frac{d^2\overline{C}}{dy^2} - sS_c\overline{C} = 0, \tag{17}$$

$$\frac{d^2\overline{F}}{dy^2} - (s+\lambda)\overline{F} + G_r\overline{T} + G_c\overline{C} = 0, \tag{18}$$

where $a = P_r/(1 + N)$, $\overline{T}(y,s) = \int_0^\infty T(y,t)e^{-st}dt$, $\overline{C}(y,s) = \int_0^\infty C(y,t)e^{-st}dt$, $\overline{F}(y,s) = \int_0^\infty F(y,t)e^{-st}dt$ and $s > 0$ (s being Laplace transform parameter).

Boundary conditions (15b)-(15f), after taking Laplace transform, become

$$\overline{F} = 1/s, \quad \overline{T} = (1 - e^{-s})/s^2, \quad \overline{C} = 1/s \quad \text{at} \quad y = 0, \tag{19a}$$

$$\overline{F} \to 0, \quad \overline{T} \to 0, \quad \overline{C} \to 0 \quad \text{as} \quad y \to \infty. \tag{19b}$$

Solution of Eqs. (16)-(18) subject to the boundary conditions (19a) and (19b) are given by

$$\overline{T}(y,s) = \frac{(1 - e^{-s})}{s^2} e^{-y\sqrt{sa}}, \tag{20}$$

$$\overline{C}(y,s) = \frac{1}{s} e^{-y\sqrt{sS_c}}, \tag{21}$$

$$\overline{F}(y,s) = \frac{1}{s} e^{-y\sqrt{s+\lambda}} + \frac{G_1(1 - e^{-s})}{s^2(s - \beta_1)}\left\{e^{-y\sqrt{s+\lambda}} - e^{-y\sqrt{sa}}\right\} + \frac{G_2}{s(s+\beta_2)}\left\{e^{-y\sqrt{s+\lambda}} - e^{-y\sqrt{sS_c}}\right\}, \tag{22}$$

where $G_1 = G_r/(a - 1)$, $G_2 = G_c/(S_c - 1)$, $\beta_1 = \lambda/(a - 1)$, $\beta_2 = \lambda/(1 - S_c)$.

Exact solution for the fluid temperature $T(y,t)$, species concentration $C(y,t)$ and fluid velocity $F(y,t)$ is obtained by taking inverse Laplace transform of the solution (20)-(22) which is expressed in the following form

$$T(y,t) = T^*(y,t) - H(t-1)T^*(y,t-1), \tag{23}$$

$$C(y,t) = erfc\left(\frac{y}{2}\sqrt{\frac{S_c}{t}}\right), \tag{24}$$

$$F(y,t) = \frac{1}{2}\left[e^{y\sqrt{\lambda}} erfc\left(\frac{y}{2\sqrt{t}} + \sqrt{\lambda t}\right) + e^{-y\sqrt{\lambda}} erfc\left(\frac{y}{2\sqrt{t}} - \sqrt{\lambda t}\right)\right] + G_1[F^*(y,t) - H(t-1)F^*(y,t-1)] + G_2 C^*(y,t), \tag{25}$$

where

$$T^*(y,t) = \left(t + \frac{ay^2}{2}\right) erfc\left(\frac{y}{2}\sqrt{\frac{a}{t}}\right) - \sqrt{\frac{at}{\pi}} y e^{-\frac{ay^2}{4t}},$$

$$\begin{aligned} F^*(y,t) = \frac{1}{2}\Bigg[\frac{e^{\beta_1 t}}{\beta_1^2}\Bigg\{ & e^{y\sqrt{(\lambda+\beta_1)}} erfc\left(\frac{y}{2\sqrt{t}} + \sqrt{(\lambda+\beta_1)t}\right) \\ & + e^{-y\sqrt{(\lambda+\beta_1)}} erfc\left(\frac{y}{2\sqrt{t}} - \sqrt{(\lambda+\beta_1)t}\right) \\ & - e^{y\sqrt{a\beta_1}} erfc\left(\frac{y}{2}\sqrt{\frac{a}{t}} + \sqrt{\beta_1 t}\right) \\ & - e^{-y\sqrt{a\beta_1}} erfc\left(\frac{y}{2}\sqrt{\frac{a}{t}} - \sqrt{\beta_1 t}\right)\Bigg\} \\ & - \frac{1}{\beta_1}\Bigg\{\left(t + \frac{1}{\beta_1} + \frac{y}{2\sqrt{\lambda}}\right) e^{y\sqrt{\lambda}} erfc\left(\frac{y}{2\sqrt{t}} + \sqrt{\lambda t}\right) \\ & + \left(t + \frac{1}{\beta_1} - \frac{y}{2\sqrt{\lambda}}\right) e^{-y\sqrt{\lambda}} erfc\left(\frac{y}{2\sqrt{t}} - \sqrt{\lambda t}\right) \\ & - 2\left(t + \frac{1}{\beta_1} + \frac{ay^2}{2}\right) erfc\left(\frac{y}{2}\sqrt{\frac{a}{t}}\right) + 2\sqrt{\frac{at}{\pi}} y e^{-\frac{ay^2}{4t}}\Bigg\}\Bigg], \end{aligned}$$

$$\begin{aligned} C^*(y,t) = \frac{1}{2\beta_2}\Bigg[& e^{y\sqrt{\lambda}} erfc\left(\frac{y}{2\sqrt{t}} + \sqrt{\lambda t}\right) + e^{-y\sqrt{\lambda}} erfc\left(\frac{y}{2\sqrt{t}} - \sqrt{\lambda t}\right) \\ & - 2 erfc\left(\frac{y}{2}\sqrt{\frac{Sc}{t}}\right) \\ & - e^{-\beta_2 t}\Bigg\{ e^{y\sqrt{\lambda-\beta_2}} erfc\left(\frac{y}{2\sqrt{t}} + \sqrt{(\lambda-\beta_2)t}\right) \\ & + e^{-y\sqrt{\lambda-\beta_2}} erfc\left(\frac{y}{2\sqrt{t}} - \sqrt{(\lambda-\beta_2)t}\right) \\ & - e^{iy\sqrt{S_c\beta_2}} erfc\left(\frac{y}{2}\sqrt{\frac{S_c}{t}} + i\sqrt{\beta_2 t}\right) \\ & - e^{-iy\sqrt{S_c\beta_2}} erfc\left(\frac{y}{2}\sqrt{\frac{S_c}{t}} - i\sqrt{\beta_2 t}\right)\Bigg\}\Bigg]. \end{aligned}$$

Here $H(t-1)$ and $erfc(x)$ are, respectively, unit step function and complementary error function.

2.1. Solution in the case of unit Schmidt number

It is noticed that solution (25) for fluid velocity is not valid for the fluids with unit Schmidt number. Schmidt number is a measure of the relative strength of viscosity to molecular (mass) diffusivity of fluid. Therefore, fluid flow problem with $S_c = 1$ corresponds to those fluids for which both viscous and concentration boundary layer thicknesses are of same order of magnitude. There are some fluids of practical interest which belong to this category [20]. Substituting $S_c = 1$ in Eq. (11) and following the same procedure as before, exact solution for species concentration $C(y,t)$ and fluid velocity $F(y,t)$ is obtained and is presented in the following form

$$C(y,t) = erfc\left(\frac{y}{2\sqrt{t}}\right), \tag{26}$$

$$\begin{aligned} F(y,t) = & \frac{1}{2}\left[e^{y\sqrt{\lambda}} erfc\left(\frac{y}{2\sqrt{t}} + \sqrt{\lambda t}\right) + e^{-y\sqrt{\lambda}} erfc\left(\frac{y}{2\sqrt{t}} - \sqrt{\lambda t}\right)\right] \\ & + G_1[F^*(y,t) - H(t-1)F^*(y,t-1)] + G_3 C_1^*(y,t), \end{aligned} \tag{27}$$

where

$G_3 = G_c/\lambda$,

$$\begin{aligned} C_1^* = \frac{1}{2}\Bigg[& \left(t + \frac{y}{2\sqrt{\lambda}}\right) e^{y\sqrt{\lambda}} erfc\left(\frac{y}{2\sqrt{t}} + \sqrt{\lambda t}\right) \\ & + \left(t - \frac{y}{2\sqrt{\lambda}}\right) e^{-y\sqrt{\lambda}} erfc\left(\frac{y}{2\sqrt{t}} - \sqrt{\lambda t}\right) - 2 erfc\left(\frac{y}{2\sqrt{t}}\right)\Bigg], \end{aligned}$$

It is noticed from the solution (24) that solution (26) for species concentration can also be deduced directly by setting $S_c = 1$ in the solution (24).

2.2. Solution in the case of Isothermal plate

Solutions (23) and (25) represent the analytical solutions for fluid temperature and fluid velocity for natural convection heat and mass transfer flow of a viscous, incompressible, electrically conducting and optically thick heat radiating fluid past an impulsively moving vertical plate with ramped temperature taking Hall current and rotation into account. In order to highlight the influence of ramped temperature distribution within the plate on the flow-field, it may be justified to compare such a flow with the one past an impulsively moving vertical plate with uniform temperature. Keeping in view the assumptions made in this paper, the solution for the fluid temperature and fluid velocity for the flow past an impulsively moving isothermal vertical plate is obtained and is presented in the following form

$$T(y,t) = erfc\left(\frac{y}{2}\sqrt{\frac{a}{t}}\right), \tag{28}$$

$$\begin{aligned} F(y,t) = \frac{(1-\gamma)}{2}\Bigg[& e^{y\sqrt{\lambda}} erfc\left(\frac{y}{2\sqrt{t}} + \sqrt{\lambda t}\right) \\ & + e^{-y\sqrt{\lambda}} erfc\left(\frac{y}{2\sqrt{t}} - \sqrt{\lambda t}\right)\Bigg] \\ & + \frac{\gamma e^{\beta_1 t}}{2}\Bigg[\Bigg\{ e^{y\sqrt{(\lambda+\beta_1)}} erfc\left(\frac{y}{2\sqrt{t}} + \sqrt{(\lambda+\beta_1)t}\right) \\ & + e^{-y\sqrt{(\lambda+\beta_1)}} erfc\left(\frac{y}{2\sqrt{t}} - \sqrt{(\lambda+\beta_1)t}\right)\Bigg\} \\ & - \Bigg\{ e^{y\sqrt{a\beta_1}} erfc\left(\frac{y}{2}\sqrt{\frac{a}{t}} + \sqrt{\beta_1 t}\right) \\ & + e^{-y\sqrt{a\beta_1}} erfc\left(\frac{y}{2}\sqrt{\frac{a}{t}} - \sqrt{\beta_1 t}\right)\Bigg\}\Bigg] \\ & + \gamma erfc\left(\frac{y}{2}\sqrt{\frac{a}{t}}\right) + G_2 C^*, \end{aligned} \tag{29}$$

where

$\gamma = G_1/\beta_1$.

2.3. Skin friction and Nusselt number

The expressions for primary skin friction τ_x, secondary skin friction τ_z and Nusselt number N_u, which are measures of shear stress at the plate due to primary flow, shear stress at the plate due to secondary flow and rate of heat transfer at the plate respectively, are presented in the following form for the ramped temperature and isothermal plates.

(i) For the ramped temperature plate

$$\tau_x + i\tau_z = \sqrt{\lambda}(erfc(\sqrt{\lambda t}) - 1) - \frac{1}{\sqrt{\pi t}}e^{-\lambda t} + G_1[F_2(0,t) - H(t-1)F_2(0,t-1)] + G_2C_2(0,t), \tag{30}$$

$$N_u = 2\sqrt{\frac{a}{\pi}}[\sqrt{t} - \sqrt{(t-1)}H(t-1)], \tag{31}$$

where

$$F_2(0,t) = \frac{e^{\beta t}}{\beta_1^2}\left[\sqrt{(\lambda+\beta_1)}\left\{erfc(\sqrt{(\lambda+\beta_1)t}) - 1\right\} - \sqrt{a\beta_1}\left\{erfc(\sqrt{\beta_1 t}) - 1\right\}\right] - \frac{1}{\beta}\left[\left\{\left(t + \frac{1}{\beta_1}\right)\sqrt{\lambda} + \frac{1}{2\sqrt{\lambda}}\right\}(erfc(\sqrt{\lambda t}) - 1) - \sqrt{\frac{t}{\pi}}(e^{-\lambda t} - \sqrt{a})\right],$$

$$C_2(0,t) = \frac{1}{\beta_2}\left[\sqrt{\lambda}(erfc(\sqrt{\lambda t}) - 1) + \frac{1}{\sqrt{\pi t}}(2\sqrt{S_c} - 1) - e^{-\beta_2 t}\left\{\sqrt{\lambda - \beta_2}(erfc\sqrt{(\lambda-\beta_2)t} - 1) - i\sqrt{S_c\beta_2}(erfc\sqrt{i\beta_2 t} - 1)\right\}\right.$$

(ii) For the isothermal plate

$$\tau_x + i\tau_z = (1-\gamma)\sqrt{\lambda}(erfc(\sqrt{\lambda t}) - 1) - \frac{1}{\sqrt{\pi t}}e^{-\lambda t} - \gamma e^{\beta t}\left\{\sqrt{(\lambda+\beta_1)}(erfc(\sqrt{(\lambda+\beta_1)t}) - 1) - \sqrt{a\beta_1}(erfc\sqrt{a\beta_1 t} - 1)\right\} - G_2C_2, \tag{32}$$

$$N_u = \sqrt{\frac{a}{t\pi}}. \tag{33}$$

It is evident from the expressions (31) and (33) that, for a given time, Nusselt number N_u is proportional to $\sqrt{a}\left(=\sqrt{\frac{P_r}{N+1}}\right)$ in both the cases i.e. Nusselt number N_u increases on increasing Prandtl number P_r while it decreases on increasing thermal radiation parameter N. Since P_r is a measure of the relative strength of viscosity to thermal diffusivity of the fluid, P_r decreases on increasing thermal diffusivity of the fluid. This implies that thermal diffusion and thermal radiation tend to reduce rate of heat transfer at both the ramped temperature and isothermal plates. Also it is noticed from (31) and (33) that N_u increases for ramped temperature plate whereas it decreases for isothermal plate on increasing time t. This implies that rate of heat transfer at ramped temperature plate is enhanced whereas it is reduced at isothermal plate with the progress of time.

2.4. Sherwood number

The expression for Sherwood number Sh, which is a measure of rate of mass transfer at the plate, is given by

$$Sh = -\sqrt{\frac{S_c}{\pi t}}. \tag{34}$$

Expression (34) reveals that Sherwood number Sh increases on increasing Schmidt number S_c and decreases on increasing time t. Since Schmidt number S_c is a measure of the relative strength of viscosity to molecular (mass) diffusivity of the fluid, S_c decreases on increasing molecular (mass) diffusivity of the fluid. Thus we conclude from (34) that mass diffusion tends to reduce rate of mass transfer at the plate and there is reduction in rate of mass transfer at the plate with the progress of time.

3. Results and discussion

In order to analyze the effects of Hall current, rotation, thermal buoyancy force, concentration buoyancy force, thermal diffusion, mass diffusion, thermal radiation and time on the flow-field, numerical values of the primary and secondary fluid velocities in the boundary layer region, computed from the analytical solutions (25) and (29), are displayed graphically versus boundary layer coordinate y in Figs. 2–17 for various values of Hall current parameter m, rotation parameter K^2, thermal Grashof number G_r, solutal Grashof number G_c, Prandtl number P_r, Schmidt number S_c, thermal radiation parameter N and time t taking magnetic parameter $M^2 = 15$

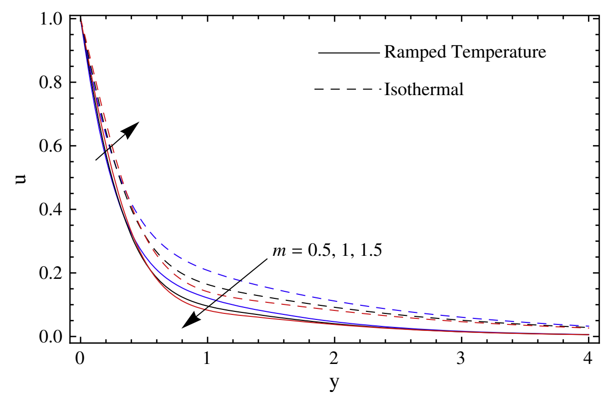

Figure 2 Primary velocity profiles when $K^2 = 5$, $G_r = 6$, $G_c = 5$, $P_r = 0.71$, $S_c = 0.6$, $N = 5$ and $t = 0.5$.

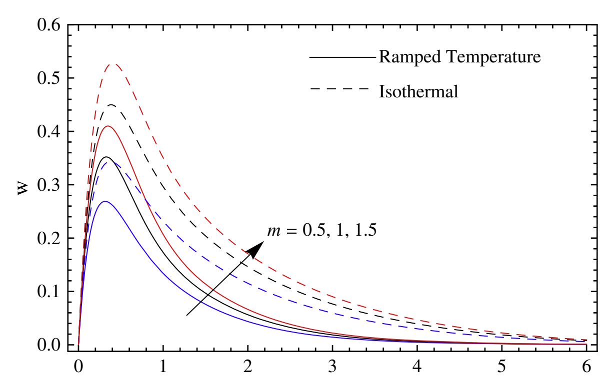

Figure 3 Secondary velocity profiles when $K^2 = 5$, $G_r = 6$, $G_c = 5$, $P_r = 0.71$, $S_c = 0.6$, $N = 5$ and $t = 0.5$.

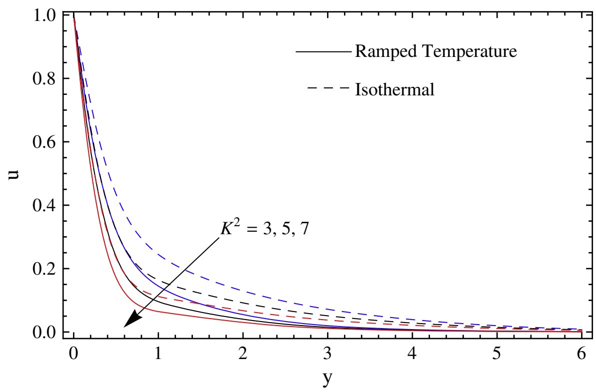

Figure 4 Primary velocity profiles when $m = 0.5$, $G_r = 6$, $G_c = 5$, $P_r = 0.71$, $S_c = 0.6$, $N = 5$ and $t = 0.5$.

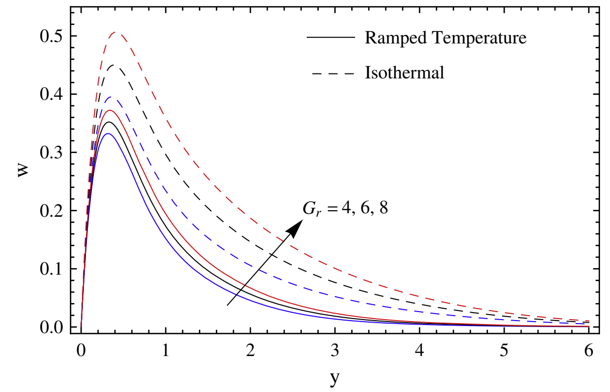

Figure 7 Secondary velocity profiles when $m = 0.5$, $K^2 = 5$, $G_c = 5$, $P_r = 0.71$, $S_c = 0.6$, $N = 5$ and $t = 0.5$.

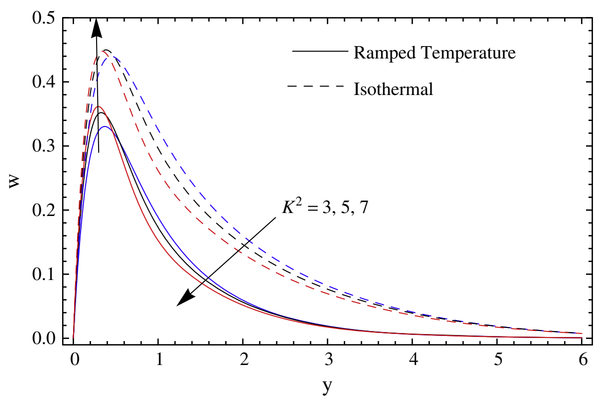

Figure 5 Secondary velocity profiles when $m = 0.5$, $G_r = 6$, $G_c = 5$, $P_r = 0.71$, $S_c = 0.6$, $N = 5$ and $t = 0.5$.

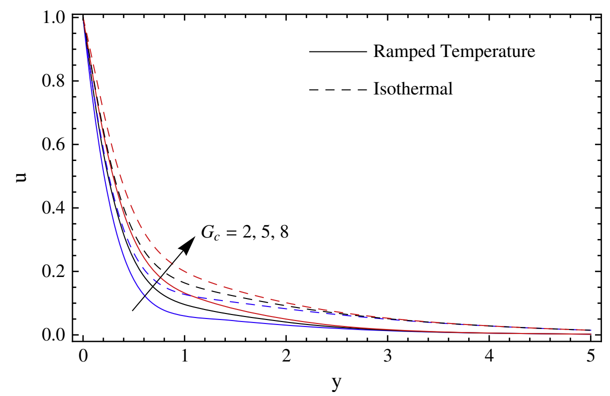

Figure 8 Primary velocity profiles when $m = 0.5$, $K^2 = 5$, $G_r = 6$, $P_r = 0.71$, $S_c = 0.6$, $N = 5$ and $t = 0.5$.

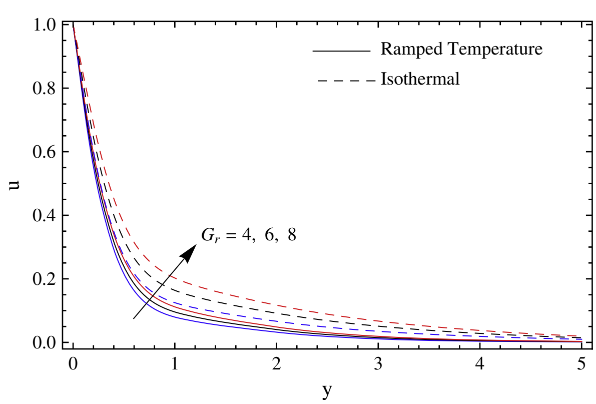

Figure 6 Primary velocity profiles when $m = 0.5$, $K^2 = 5$, $G_c = 5$, $P_r = 0.71$, $S_c = 0.6$, $N = 5$ and $t = 0.5$.

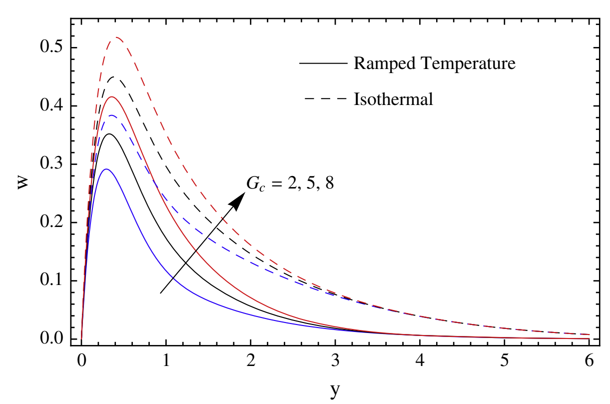

Figure 9 Secondary velocity profiles when $m = 0.5$, $K^2 = 5$, $G_r = 6$, $P_r = 0.71$, $S_c = 0.6$, $N = 5$ and $t = 0.5$.

and permeability parameter $K_1 = 0.4$. It is revealed from Figs. 2–17 that, for both ramped temperature and isothermal plates, primary velocity u and secondary velocity w attain a distinctive maximum value near surface of the plate and then decrease properly on increasing boundary layer coordinate y to approach free stream value. It is also noticed that the primary and secondary fluid velocities are slower in the case of ramped temperature plate than that of isothermal plate.

Figs. 2 and 3 depict the influence of Hall current on the primary velocity u and secondary velocity w for both ramped temperature and isothermal plates. It is evident from Figs. 2 and 3 that, for both ramped temperature and isothermal plates, u increases on increasing m in a region near to the plate and it decreases on increasing m in the region away from the plate whereas w increases on increasing m throughout the boundary layer region. This implies that, for both ramped temperature

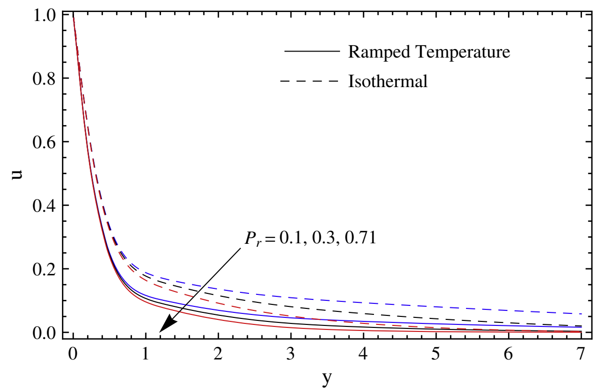

Figure 10 Primary velocity profiles when $m = 0.5$, $K^2 = 5$, $G_r = 6$, $G_c = 5$, $S_c = 0.6$, $N = 5$ and $t = 0.5$.

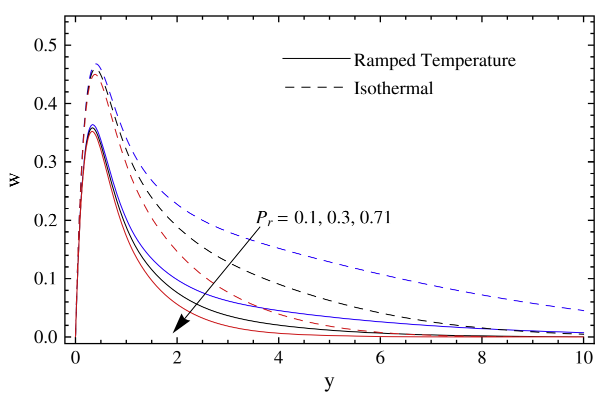

Figure 11 Secondary velocity profiles when $m = 0.5$, $K^2 = 5$, $G_r = 6$, $G_c = 5$, $S_c = 0.6$, $N = 5$ and $t = 0.5$.

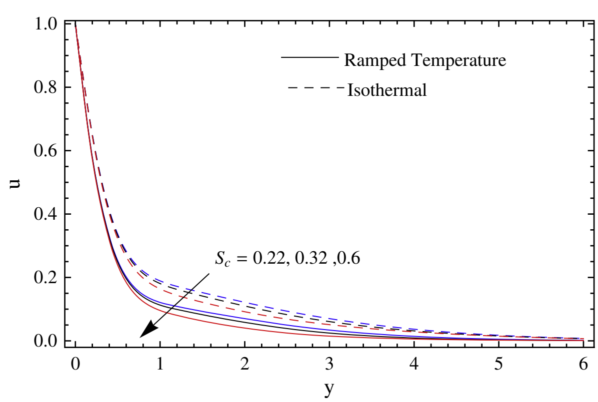

Figure 12 Primary velocity profiles when $m = 0.5$, $K^2 = 5$, $G_r = 6$, $G_c = 5$, $P_r = 0.71$, $N = 5$ and $t = 0.5$.

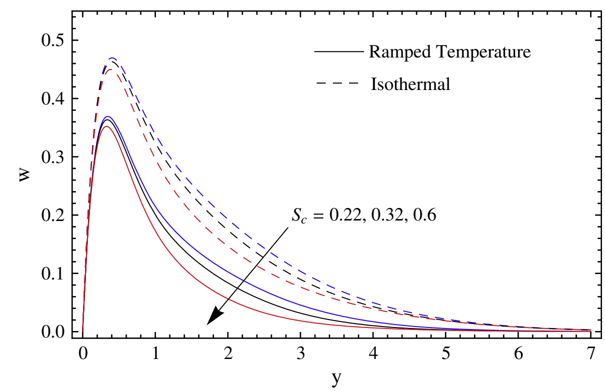

Figure 13 Secondary velocity profiles when $m = 0.5$, $K^2 = 5$, $G_r = 6$, $G_c = 5$, $P_r = 0.71$, $N = 5$ and $t = 0.5$.

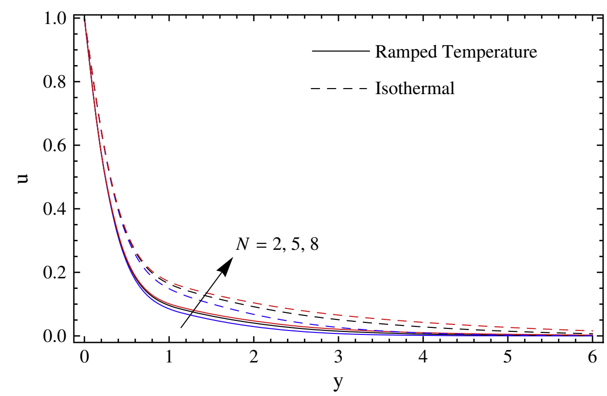

Figure 14 Primary velocity profiles when $m = 0.5$, $K^2 = 5$, $G_r = 6$, $G_c = 5$, $P_r = 0.71$, $S_c = 0.6$ and $t = 0.5$.

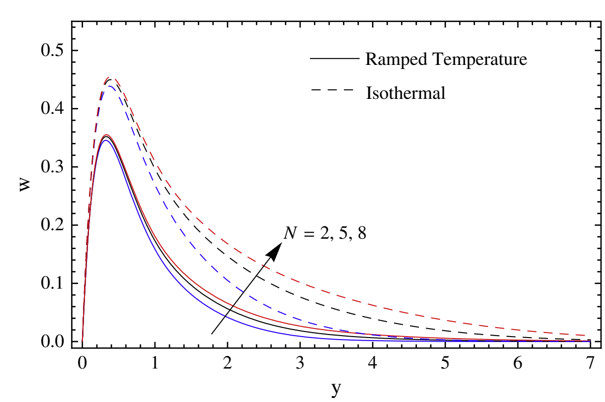

Figure 15 Secondary velocity profiles when $m = 0.5$, $K^2 = 5$, $G_r = 6$, $G_c = 5$, $P_r = 0.71$, $S_c = 0.6$ and $t = 0.5$.

and isothermal plates, Hall current tends to accelerate secondary fluid velocity throughout the boundary layer region which is consistent with the fact that Hall current induces secondary flow in the flow-field. Hall current tends to accelerate primary fluid velocity in a region close to the plate whereas it has a reverse effect on primary fluid velocity in the region away from the plate. Figs. 4 and 5 illustrate the effects of rotation on the primary and secondary fluid velocities for both ramped temperature and isothermal plates. It is perceived from Figs. 4 and 5 that, for both ramped temperature and isothermal plates, u decreases on increasing K^2 whereas w increases on increasing K^2 in the region near to the plate and it decreases on increasing K^2 in the region away from the plate. This implies that, for both ramped temperature and isothermal plates, rotation tends to retard primary fluid velocity throughout the boundary layer region. Although rotation is known to induce

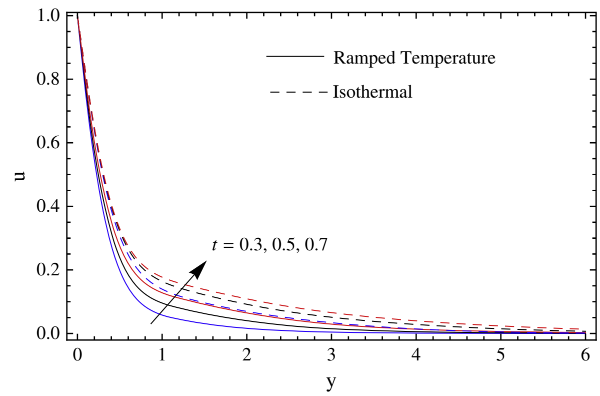

Figure 16 Primary velocity profiles when $m = 0.5$, $K^2 = 5$, $G_r = 6$, $G_c = 5$, $P_r = 0.71$, $S_c = 0.6$ and $N = 5$.

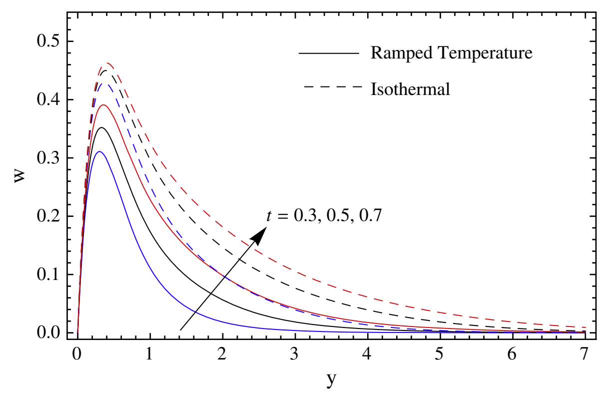

Figure 17 Secondary velocity profiles when $m = 0.5$, $K^2 = 5$, $G_r = 6$, $G_c = 5$, $P_r = 0.71$, $S_c = 0.6$ and $N = 5$.

secondary fluid velocity in the flow-field by suppressing the primary fluid velocity, its accelerating effect is prevalent only in the region near to the plate whereas it has a reverse effect on secondary fluid velocity in the region away from the plate. This is due to the reason that Coriolis force is dominant in the region near to the axis of rotation. Figs. 6–9 demonstrate the effects of thermal and concentration buoyancy forces on the primary and secondary fluid velocities for both ramped temperature and isothermal plates. It is revealed from Figs. 6–9 that, for both ramped temperature and isothermal plates, u and w increase on increasing G_r and G_c. G_r represents the relative strength of thermal buoyancy force to viscous force and G_c represents the relative strength of concentration buoyancy force to viscous force. Therefore, G_r and G_c increase on increasing the strengths of thermal and concentration buoyancy forces respectively. In this problem natural convection flow is induced due to thermal and concentration buoyancy forces, therefore thermal and concentration buoyancy forces tend to accelerate primary and secondary fluid velocities throughout the boundary layer region for both ramped temperature and isothermal plates which is clearly evident from Figs. 6–9. Figs. 10–13 depict the influence of thermal and mass diffusions on the primary and secondary fluid velocities for both ramped temperature and isothermal plates. It is noticed from Figs. 10–13 that, for both ramped temperature and isothermal plates, u and w decrease on increasing P_r and S_c. This implies that thermal and mass diffusions tend to accelerate primary and secondary fluid velocities throughout the boundary layer region for both ramped temperature and isothermal plates which happens due to the fact that thermal and mass diffusions provide an impetus to the thermal and concentration buoyancy forces respectively. Figs. 14 and 15 present the effects of thermal radiation on the primary and secondary fluid velocities for both ramped temperature and isothermal plates. It is evident from Figs. 14 and 15 that, for both ramped

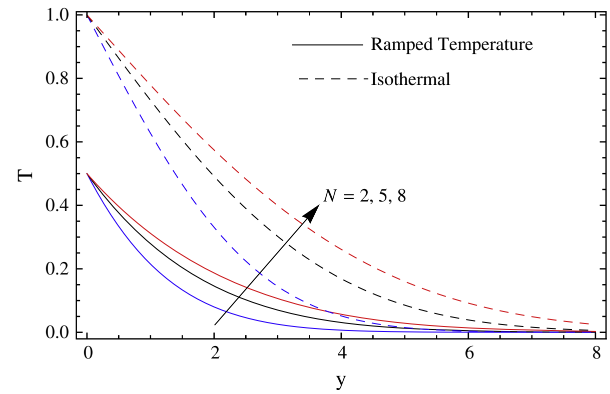

Figure 18 Temperature profiles when $P_r = 0.71$ and $t = 0.5$.

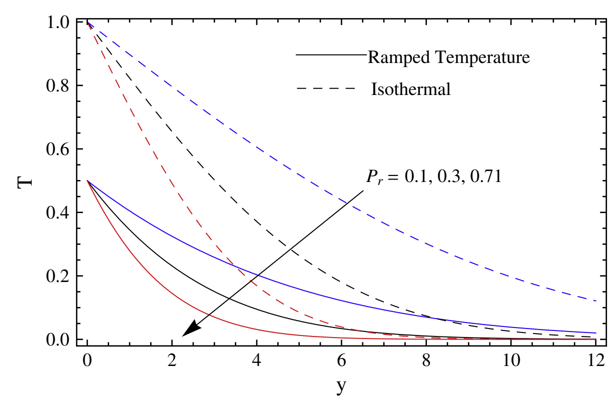

Figure 19 Temperature profiles when $N = 5$ and $t = 0.5$.

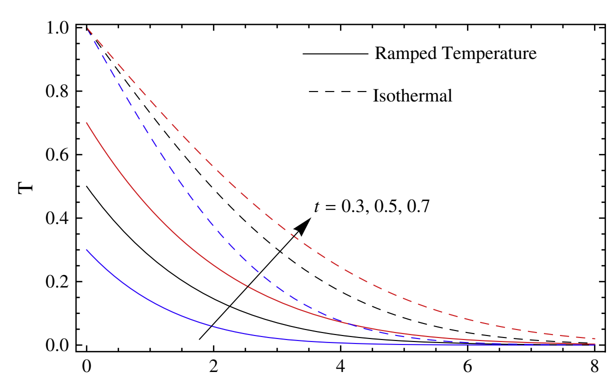

Figure 20 Temperature profiles when $N = 5$ and $P_r = 0.71$.

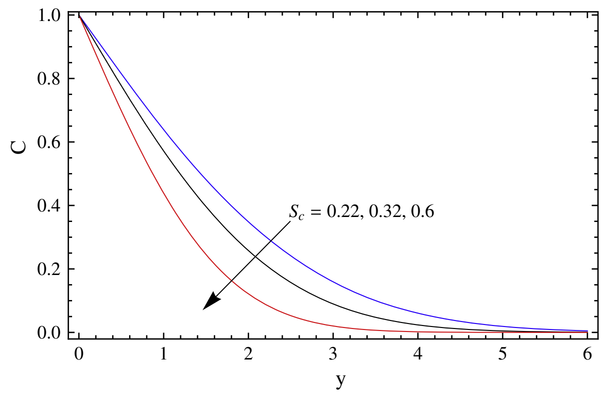

Figure 21 Concentration profiles when $t = 0.5$.

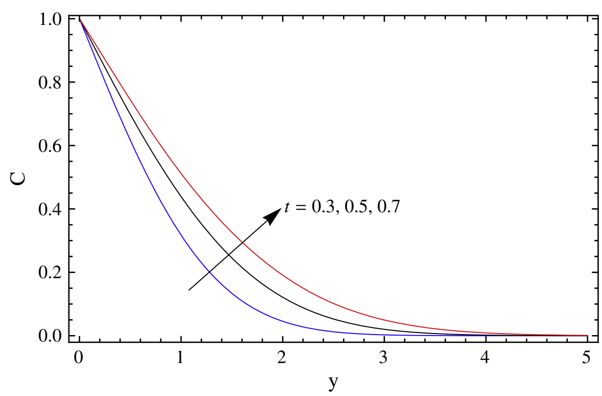

Figure 22 Concentration profiles when $S_c = 0.6$.

temperature and isothermal plates, u and w increase on increasing N. This implies that thermal radiation tends to accelerate primary and secondary fluid velocities throughout the boundary layer region for both ramped temperature and isothermal plates. Figs. 16 and 17 present the influence of time on the primary and secondary fluid velocities for both ramped temperature and isothermal plates. It is evident from Figs. 16 and 17 that, for both ramped temperature and isothermal plates, u and w increase on increasing t. This implies that primary and secondary fluid velocities are getting accelerated with the progress of time throughout the boundary layer region for both ramped temperature and isothermal plates. Thus it may be concluded that thermal and concentration buoyancy forces, thermal and mass diffusions and thermal radiation tend to increase the thickness of modified Ekmann–Hartmann boundary layer for both ramped temperature and isothermal plates. Thickness of modified Ekmann–Hartmann boundary layer also increases with the progress of time.

The numerical values of fluid temperature T, computed from the analytical solutions (23) and (28), are depicted graphically versus boundary layer coordinate y in Figs. 18–20 for various values of N, P_r and t. It is evident from Fig. 18 that fluid temperature T increases on increasing N for both ramped temperature and isothermal plates. Thus thermal radiation tends to enhance fluid temperature throughout the boundary layer region for both ramped temperature and isothermal plates. This is consistent with the fact that thermal radiation provides an additional means to diffuse energy because thermal radiation parameter $N = 16\sigma^* T_\infty'^3/3kk^*$ and, therefore, an increase in N implies a decrease in Rosseland mean absorption coefficient k^* for fixed values of T'_∞ and k. Figs. 19 and 20 reveal that fluid temperature T decreases on increasing P_r whereas it increases on increasing t for both ramped temperature and isothermal plates. This implies that, for both ramped temperature and isothermal plates, thermal diffusion tends to enhance fluid temperature and there is an enhancement in fluid temperature with the progress of time throughout the boundary layer region.

The numerical values of species concentration C, computed from the analytical solution (24), are presented graphically versus boundary layer coordinate y in Figs. 21 and 22 for various values of Schmidt number S_c and time t. It is evident from Figs. 21 and 22 that species concentration C decreases on increasing S_c whereas it increases on increasing t. This implies that mass diffusion tends to enhance species concentration and there is an enhancement in species concentration with the progress of time throughout the boundary layer region.

The numerical values of primary skin friction τ_x, secondary skin friction τ_z, computed from analytical expressions (30) and

Table 1 Skin Friction for ramped temperature plate when $G_r = 6$, $G_c = 5$, $S_c = 0.6$, $P_r = 0.71$, $N = 5$ and $t = 0.5$.

$m\downarrow$ $K^2\rightarrow$	$-\tau_x$			τ_z		
	3	5	7	3	5	7
0.5	2.61086	2.87124	3.14162	1.86439	2.35018	2.77199
1	2.13978	2.49195	2.82669	2.39783	2.85995	3.24915
1.5	1.71334	2.13659	2.52149	2.6113	3.06904	3.44657

Table 2 Skin Friction for isothermal plate when $G_r = 6$, $G_c = 5$, $S_c = 0.6$, $P_r = 0.71$, $N = 5$ and $t = 0.5$.

$m\downarrow$ $K^2\rightarrow$	$-\tau_x$			τ_z		
	3	5	7	3	5	7
0.5	1.97001	2.29044	2.61276	2.09575	2.60816	3.04199
1	1.49712	1.92406	2.31628	2.72375	3.19048	3.57514
1.5	1.05478	1.56425	2.01173	3.00567	3.45031	3.8123

(32), are presented in tabular form in Tables 1–8 for various values of m, K^2, G_r, G_c, P_r, S_c, N and t taking $M^2 = 15$ and $K_1 = 0.4$. It is evident from Tables 1–8 that primary skin friction τ_x decreases on increasing m, G_r, G_c, N and t whereas it increases on increasing K^2, P_r and S_c for both ramped temperature and isothermal plates. Secondary skin friction τ_z

Table 3 Skin Friction for ramped temperature plate when $m = 0.5$, $K^2 = 5$, $S_c = 0.6$, $P_r = 0.71$, $N = 5$ and $t = 0.5$.

$G_r\downarrow$ $G_c\rightarrow$	$-\tau_x$			τ_z		
	2	5	8	2	5	8
4	3.54881	3.05691	2.56502	2.12728	2.27855	2.42982
6	3.36313	2.87124	2.37934	2.19891	2.35018	2.50144
8	3.17746	2.68556	2.19367	2.27053	2.4218	2.57307

Table 4 Skin Friction for isothermal plate when $m = 0.5$, $K^2 = 5$, $S_c = 0.6$, $P_r = 0.71$, $N = 5$ and $t = 0.5$.

$G_r\downarrow$ $G_c\rightarrow$	$-\tau_x$			τ_z		
	2	5	8	2	5	8
4	3.16161	2.66971	2.17782	2.29927	2.45054	2.60181
6	2.78234	2.29044	1.79854	2.45689	2.60816	2.75943
8	2.40306	1.91117	1.41927	2.61452	2.76579	2.91706

Table 5 Skin Friction for ramped temperature plate when $m = 0.5$, $K^2 = 5$, $G_r = 6$, $G_c = 5$, $N = 5$ and $t = 0.5$.

$P_r\downarrow$ $S_c\rightarrow$	$-\tau_x$			τ_z		
	0.22	0.32	0.6	0.22	0.32	0.6
0.1	2.74295	2.77893	2.85691	2.48513	2.44529	2.36022
0.3	2.74947	2.78546	2.86344	2.48015	2.44032	2.35524
0.71	2.75727	2.79326	2.87124	2.47509	2.43525	2.35018

Table 6 Skin Friction for isothermal plate when $m = 0.5$, $K^2 = 5$, $G_r = 6$, $G_c = 5$, $N = 5$ and $t = 0.5$.

$P_r\downarrow$ $S_c\rightarrow$	$-\tau_x$			τ_z		
	0.22	0.32	0.6	0.22	0.32	0.6
0.1	2.13976	2.17575	2.25373	2.77629	2.73645	2.65137
0.3	2.1518	2.18779	2.26577	2.76208	2.72224	2.63716
0.71	2.17647	2.21246	2.29044	2.73308	2.69324	2.60816

Table 7 Skin Friction for ramped temperature plate when $m = 0.5$, $K^2 = 5$, $G_r = 6$, $G_c = 5$, $S_c = 0.6$and $P_r = 0.71$.

$N\downarrow$ $t\rightarrow$	$-\tau_x$			τ_z		
	0.3	0.5	0.7	0.3	0.5	0.7
2	3.15529	2.8797	2.6249	2.1961	2.34589	2.47178
5	3.14916	2.87124	2.61451	2.19751	2.35018	2.47832
8	3.14616	2.86722	2.60964	2.19868	2.35266	2.48183

Table 8 Skin Friction for isothermal plate when $m = 0.5$, $K^2 = 5$, $G_r = 6$, $G_c = 5$, $S_c = 0.6$ and $P_r = 0.71$.

$N\downarrow$ $t\rightarrow$	$-\tau_x$			τ_z		
	0.3	0.5	0.7	0.3	0.5	0.7
2	2.371	2.30825	2.27385	2.5094	2.58784	2.62882
5	2.34861	2.29044	2.25878	2.53685	2.60816	2.64585
8	2.33898	2.28258	2.25212	2.54949	2.61729	2.65348

increases on increasing m, K_2, G_r, G_c, Nandt whereas it decreases on increasing P_r and S_c for both ramped temperature and isothermal plates. This implies that, for both ramped temperature and isothermal plates, Hall current, thermal buoyancy force, concentration buoyancy force, thermal and mass diffusions and thermal radiation have tendency to reduce primary skin friction whereas these physical quantities have reverse effect on secondary skin friction. Rotation tends to enhance both the primary and secondary skin frictions for both ramped temperature and isothermal plates. As time progresses, primary skin friction is getting reduced whereas secondary skin friction is getting enhanced for both ramped temperature and isothermal plates.

4. Conclusions

An investigation of the effects of Hall current and rotation on unsteady hydromagnetic natural convection flow with heat and mass transfer of a viscous, incompressible, electrically conducting and optically thick radiating fluid past an impulsively moving vertical plate embedded in a fluid saturated porous medium, when temperature of the plate has a temporarily ramped profile, is carried out. Significant findings are as follows:

For both ramped temperature and isothermal plates

- Hall current tends to accelerate secondary fluid velocity throughout the boundary layer region. Hall current tends to accelerate primary fluid velocity in a region close to the plate whereas it has a reverse effect on the primary fluid velocity in the region away from the plate.
- Rotation tends to retard primary fluid velocity throughout the boundary layer region. Rotation tends to accelerate secondary fluid velocity only in the region near to the plate whereas it has a reverse effect on secondary fluid velocity in the region away from the plate.
- Thermal and concentration buoyancy forces, thermal and mass diffusions and thermal radiation tend to accelerate both the primary and secondary fluid velocities throughout the boundary layer region.
- Primary and secondary fluid velocities are getting accelerated with the progress of time throughout the boundary layer region.
- Thermal radiation and thermal diffusion tend to enhance fluid temperature and there is an enhancement in fluid temperature with the progress of time throughout the boundary layer region.
- Mass diffusion tends to enhance species concentration and there is an enhancement in species concentration with the progress of time throughout the boundary layer region.
- Hall current, thermal and concentration buoyancy forces, thermal and mass diffusions and thermal radiation have tendency to reduce primary skin friction whereas these physical quantities have reverse effect on secondary skin friction.
- Rotation tends to enhance both the primary and secondary skin frictions.
- Primary skin friction is getting reduced whereas secondary skin friction is getting enhanced with the progress of time.

Acknowledgement

Authors are grateful to the reviewers for their valuable suggestions and comments which helped them to improve the quality of this research paper.

References

[1] Bejan A. Convection heat transfer. 2nd ed. NY: Wiley; 1993.
[2] Gebhart B, Pera L. The nature of vertical natural convection flows resulting from the combined buoyancy effects of thermal and mass diffusion. Int J Heat Mass Transfer 1971;14:2025–50.
[3] Raptis AA. Free convection and mass transfer effects on the oscillatory flow past an infinite moving vertical isothermal plate with constant suction and heat sources. Astrophy Space Sci 1982;86:43–53.
[4] Bejan A, Khair KR. Heat and mass transfer by natural convection in a porous medium. Int J Heat Mass Transfer 1985;28:909–18.
[5] Jang JY, Chang WJ. Buoyancy-induced inclined boundary layer flow in a porous medium resulting from combined heat and mass buoyancy effects. Int Commun Heat Mass Transfer 1988;15:17–30.
[6] Lai FC, Kulacki FA. Non-Darcy mixed convection along a vertical wall in a saturated porous medium. J Heat Transfer 1991;113:252–5.
[7] Nakayama A, Hossain MA. An integral treatment for combined heat and mass transfer by natural convection in a porous medium. Int J Heat Mass Transfer 1995;38:761–5.
[8] Yih KA. The effect of transpiration on coupled heat and mass transfer in mixed convection over a vertical plate embedded in a saturated porous medium. Int Commun Heat Mass Transfer 1997;24:265–75.
[9] Chamkha AJ, Takhar HS, Soundalgekar VM. Radiation effects on free convection flow past a semi-infinite vertical plate with mass transfer. Chem Eng J 2001;84:335–42.
[10] Ganesan P, Palani G. Natural convection effects on impulsively started inclined plate with heat and mass transfer. Heat Mass Transfer 2003;39:277–83.
[11] Eckert ER, Drake RM. Analysis of heat and mass transfer. NY: Mc-Graw Hill; 1972.
[12] Gebhart B, Jaluria Y, Mahajan RL, Sammakia B. Buoyancy Induced Flow and Transport, New York Hemisphere; 1998.
[13] Nield DA, Bejan A. Convection in porous media. 3rd ed. NY: Springer; 2006.
[14] Pop I, Ingham DB. Convective heat transfer: mathematical and computational modelling of viscous fluids and porous media. Oxford: Pergamon; 2001.
[15] Incropera FP, Bergman TL, Lavine AS, Dewitt DP. Fundamentals of heat and mass transfer. NY: John Wiley & Sons; 2011.
[16] Oreper GM, Szekely J. The effect of an externally imposed magnetic field on buoyancy driven flow in a rectangular cavity. J Cryst Growth 1983;64:505–15.
[17] Hossain MA, Mandal AC. Mass transfer effects on the unsteady hydromagnetic free convection flow past an accelerated vertical porous plate. J Phys D: Appl Phys 1985;18:163–9.
[18] Jha BK. MHD free convection and mass transform flow through a porous medium. Astrophys Space Sci 1991;175:283–9.
[19] Elbashbeshy EMA. Heat and mass transfer along a vertical plate with variable surface tension and concentration in the presence of the magnetic field. Int J Eng Sci 1997;35:515–22.
[20] Chen CH. Combined heat and mass transfer in MHD free convection from a vertical surface with Ohmic heating and viscous dissipation. Int J Eng Sci 2004;42:699–713.
[21] Ibrahim FS, Hassanien IA, Bakr AA. Unsteady magnetohydrodynamic micropolar fluid flow and heat transfer over a vertical

porous plate through a porous medium in the presence of thermal and mass diffusion with a constant heat source. Can J Phys 2004;82:775–90.
[22] Chamkha AJ. Unsteady MHD convective heat and mass transfer past a semi-infinite vertical permeable moving plate with heat absorption. Int J Eng Sci 2004;42:217–30.
[23] Makinde OD, Sibanda P. Magnetohydrodynamic mixed convective flow and heat and mass transfer past a vertical plate in a porous medium with constant wall suction. J Heat Transfer 2008;130:8 [Article No. 112602].
[24] Makinde OD. On MHD boundary layer flow and mass transfer past a vertical plate in a porous medium with constant heat flux. Int J Numer Methods Heat Fluid Flow 2009;19:546–54.
[25] Eldabe NTM, Elbashbeshy EMA, Hasanin WSA, Elsaid EM. Unsteady motion of MHD viscous incompressible fluid with heat and mass transfer through porous medium near a moving vertical plate. Int J Energy Tech 2011;3(35):1–11.
[26] Singh AK. MHD free-convection flow in the stokes problem for a vertical porous plate in a rotating system. Astrophys Space Sci 1983;95(2):283–9.
[27] Singh AK. MHD free convection flow past an accelerated vertical porous plate in a rotating fluid. Astrophys Space Sci 1984;103:155–63.
[28] Raptis AA, Singh AK. Rotation effects on MHD free-convection flow past an accelerated vertical plate. Mech Res Commun 1985;12(1):31–40.
[29] Kythe PK, Puri P. Unsteady MHD free convection flows on a porous plate with time-dependent heating in a rotating medium. Astrophys Space Sci 1988;143(1):51–62.
[30] Tokis JN. Free convection and mass transfer effects on the magnetohydrodynamic flows near a moving plate in a rotating medium. Astrophys Space Sci 1988;144:291–301.
[31] Nanousis N. Thermal diffusion effects on MHD free convective and mass transfer flow past a moving infinite vertical plate in a rotating fluid. Astrophys Space Sci 1992;191(2):313–22.
[32] Singh AK, Singh NP, Singh U, Singh H. Convective flow past an accelerated porous plate in rotating system in presence of magnetic field. Int J Heat Mass Transfer 2009;52:3390–5.
[33] Seddeek MA. Effects of radiation and variable viscosity on a MHD free convection flow past a semi-infinite flat plate with an aligned magnetic field in the case of unsteady flow. Int J Heat Mass Transfer 2002;45:931–5.
[34] Viskanta R, Grosh RJ. Boundary layer in thermal radiation absorbing and emitting media. Int J Heat Mass Transfer 1962;5:795–806.
[35] Cess RD. The interaction of thermal radiation with free convection heat transfer. Int J Heat Mass Transfer 1966;9:1269–77.
[36] Sparrow EM, Cess RD. Radiation heat transfer. Belmont, Calif.: Brooks/Cole; 1966.
[37] Howell JR, Siegel R, Mengüç MP. Thermal radiation heat transfer. 5th ed. FL: CRC Press; 2010.
[38] Takhar HS, Gorla RSR, Soundalgekar VM. Short communication radiation effects on MHD free convection flow of a gas past a semi-infinite vertical plate. Int J Numer Methods Heat Fluid Flow 1996;6:77–83.
[39] Raptis A, Massalas CV. Magnetohydrodynamic flow past a plate by the presence of radiation. Heat Mass Transfer 1998;34:107–9.
[40] Chamkha AJ. Thermal radiation and buoyancy effects on hydromagnetic flow over an accelerating permeable surface with heat source or sink. Int J Eng Sci 2000;38:1699–712.
[41] Cookey CI, Ogulu A, Omubo-Pepple VB. Influence of viscous dissipation and radiation on unsteady MHD free convection flow past an infinite heated vertical plate in a porous medium with time-dependent suction. Int J Heat Mass Transfer 2003;46:2305–11.
[42] Suneetha S, Bhaskar Reddy N, Ramachandra Prasad V. Thermal radiation effects on MHD free convection flow past an impulsively started vertical plate with variable surface temperature and concentration. J Naval Archit Marine Eng 2008;5(2):57–70.
[43] Ogulu A, Makinde OD. Unsteady hydromagnetic free convection flow of a dissipative and radiating fluid past a vertical plate with constant heat flux. Chem Eng Commun 2008;196:454–62.
[44] Mahmoud MAA. Thermal radiation effect on unsteady MHD free convection flow past a vertical plate with temperature dependent viscosity. Can J Chem Eng 2009;87:47–52.
[45] Schetz JA. On the approximate solution of viscous flow problems. J Appl Mech 1963;30:263–8.
[46] Schetz JA, Eichhorn R. Natural convection with discontinuous wall-temperature variations. J Fluid Mech 1964;18:167–76.
[47] Hayday AA, Bowlus DA, McGraw RA. Free convection from a vertical plate with step discontinuities in surface temperature. J Heat Transfer 1967;89:244–9.
[48] Kelleher M. Free convection from a vertical plate with discontinuous wall temperature. J Heat Transfer 1971;93:349–56.
[49] Kao TT. Laminar free convective heat transfer response along a vertical flat plate with step jump in surface temperature. Lett Heat Mass Transfer 1975;2:419–28.
[50] Lee S, Yovanovich MM. Laminar natural convection from a vertical plate with a step change in wall temperature. J Heat Transfer 1991;113:501–4.
[51] Chandran P, Sacheti NC, Singh AK. Natural convection near a vertical plate with ramped wall temperature. Heat Mass Transfer 2005;41:459–64.
[52] Patra RR, Das S, Jana RN, Ghosh SK. Transient approach to radiative heat transfer free convection flow with ramped wall temperature. J Appl Fluid Mech 2012;5:9–13.
[53] Narahari M. Transient free convection flow between long vertical parallel plates with ramped wall temperature at one boundary in the presence of thermal radiation and constant mass diffusion. Meccanica 2012;47:1961–76.
[54] Seth GS, Ansari MdS, Nandkeolyar R. MHD natural convection flow with radiative heat transfer past an impulsively moving plate with ramped wall temperature. Heat Mass Transfer 2011;47:551–61.
[55] Seth GS, Nandkeolyar R, Ansari MdS. Effects of thermal radiation and rotation on unsteady hydromagnetic free convection flow past an impulsively moving vertical plate with ramped temperature in a porous medium. J Appl Fluid Mech 2013;6:27–38.
[56] Pop I, Watanabe T. Hall effect on magnetohydrodynamic free convection about a semi-infinite vertical flat plate. Int J Eng Sci 1994;32:1903–11.
[57] Abo-Eldahab EM, Elbarbary EME. Hall current effect on magnetohydrodynamic free-convection flow past a semi-infinite vertical plate with mass transfer. Int J Eng Sci 2001;39:1641–52.
[58] Takhar HS, Roy S, Nath G. Unsteady free convection flow over an infinite vertical porous plate due to the combined effects of thermal and mass diffusion, magnetic field and Hall currents. Heat Mass Transfer 2003;39:825–34.
[59] Saha LK, Siddiqa S, Hossain MA. Effect of Hall current on MHD natural convection flow from vertical permeable flat plate with uniform surface heat flux. Appl Math Mech Engl Ed 2011;32(9):1127–46.
[60] Satya Narayana PV, Venkateswarlu B, Venkataramana S. Effects of Hall current and radiation absorption on MHD micropolar fluid in a rotating system. Ain Shams Eng J 2013;4:843–54.
[61] Seth GS, Mahato GK, Sarkar S. Effects of Hall current and rotation on MHD natural convection flow past an impulsively moving vertical plate with ramped temperature in the presence of thermal diffusion with heat absorption. Int J Energy Tech 2013;5(16):1–12.
[62] Cramer KR, Pai SI. Magnetofluid dynamics for engineers and applied physicists. NY: McGraw Hill Book Company; 1973.

G.S. Seth is a Professor in the Department of Applied Mathematics, Indian School of Mines, Dhanbad, India. He received his Ph.D. in the Mathematics from Indian Institute of Technology, Kharagpur, India. He has more than thirty three years of experience of teaching and research. His current area of research studies includes Fluid dynamics, Magnetohydrodynamics and heat and mass transfer. He was visiting Assistant Professor at University of Aden, Republic of Yemen during the period September 01, 1991 to August 31, 1993. He has published more than seventy seven research papers in national/International journals of repute.

S. Sarkar has done B.Sc. in Mathematics from Presidency College, Kolkata, India. He has received M.Sc. Degree in Mathematics and Computing from Indian School of Mines, Dhanbad in 2010. He has received M.Phil degree in Applied Mathematics from Indian School of Mines, Dhanbad in 2011. In the year 2012, he has joined Department of Applied Mathematics, Indian School of Mines, Dhanbad as a full time research fellow to do research work leading to Ph.D. degree. He has 2 years of research experience. He has published eight research papers in peer reviewed International Journals of repute.

S.M. Hussain received M.Sc. Degree in Mathematics from Vinova Bhave University, Hazaribag, Jharkhand in 2008. He received M.Phil degree in Applied Mathematics from Indian School of Mines, Dhanbad in 2009. He joined O.P. Jindal Institute of Technology, Raigarh, India as an Assistant Professor in the Department of Mathematics in 2009. In the year 2011, he has joined as a research scholar in the Department of Applied Mathematics to do the research work leading to Ph.D. He has 4 years of teaching experience and 3 years of research experience. He has published six research papers in the peer reviewed International Journals of repute.